Theoretical Studies of Decomposition Reactions of Dioxetane, Dioxetanone, and Related Species. CT Induced Luminescence Mechanism Revisited

Yu Takano, Tsunaki Tsunesada, Hiroshi Isobe, Yasunori Yoshioka, Kizashi Yamaguchi,* and Isao Saito†,#

Department of Chemistry, Graduate School of Science, Osaka University, Toyonaka, Osaka 560-0043

†Department of Chemistry, Graduate School of Engineering, Kyoto University, Sakyo-ku, Kyoto 606-8224

(Received August 24, 1998)

The electronic structures and relative stabilities of homopolar biradicals (BR) and CT BR with significant one-electron transfer (ET) BR characters were investigated by ab initio MO calculations. The previously presented inter- and intramolecular CT models were extended in order to elucidate possible mechanisms for decomposition reactions of dioxetane, dioxetanone, and related species. The computational results indicate that endothermic O–O cleavages, followed by charge-transfers, are operative for the chemiluminescence reactions of these peroxides with several anionic species, in contradiction to the chemically initiated electron-exchange luminescence (CIEEL) mechanism, where complete one-electron transfer (ET) is required for the formation of excited carbonyl fragments. The ionization potentials of monoanions of phenol, indole and luciferins were calculated semiempirically in order to estimate the CT excitation energies from these species to the O–O antibonding orbital. The CT excitation energies are used to distinguish between the CT induced luminescence (CTIL) mechanism and the CIEEL mechanism for chemiluminescence reactions. Orbital-interaction models are also presented to explain of the so-called odd/even selection rule for the efficiency of chemiluminescence reactions. The implications of these results are discussed in relation to recent experimental results, together with biological chemiluminescence reactions of luciferins and related species.

The thermal decompositions of dioxetanes, dioxetanones, and related species have been extensively investigated in relation to the mechanisms of chemi- and bio-luminescence reactions.[1—3] These luminescence reactions have also been attractive from the view point of diagnostic clinical applications.[4] Therefore, several theoretical studies have already been carried out to elucidate possible mechanisms of the luminescence reactions. The simple MO correlation diagrams by Kearns[5] indicated that a symmetry allowed (concerted) decomposition of dioxetane occurs to afford the excited carbonyl compound. This mechanism is compatible with McCapa's proposal.[6] Kearns, however, pointed out that the homolytic O–O cleavage, affording a 1,6-biradical, occurs preferentially in the retro Diels–Alder reaction of endoperoxide, because of the instability of the O–O bond. Boche and Runquist[7] have shown that the O–O homolysis indeed occurs in the case of ascaridole. Richardson and O'Neal[8] have proposed a biradical mechanism for dioxetane decompositions on thermochemical grounds. Several experimental results[1—3] are also compatible with a two-step mechanism involving a 1,4-biradical.

We previously examined the triplet instability of the restricted Hartree–Fock (RHF) solution during the course of the dissociation reaction of dioxetane.[9] It was found that the RHF MO is highly unstable, and can be reorganized into the different orbitals for different spins (DODS) MO's,[10] which are given by strong mixing of the bonding and antibonding O–O σ-orbitals of dioxetane. The orbital phase relations changed during the course of O–O dissociation, because of MO mixing, showing the orbital symmetry-forbidden character. From a symmetry-stability analysis, the symmetry-forbidden biradical (FR) mechanism was concluded for the thermolysis of dioxetane.[9] Hilal reached a similar conclusion that the two different RHF (6-31G) solutions are degenerate in energy at the orbital crossing point.[11] On the basis of the generalized valence-bond (GVB) plus thermochemical calculations, Harding and Goddard[12] also concluded the biradical (BR) mechanism for the O–O homolysis of dioxetane. Recently, Reguero et al.[13] located the transition structure for the decomposition of dioxetane by the complete active space (CAS) self-consistent field (SCF) energy-gradient technique, showing the homopolar BR transition state (TS). Thus, theoretical models involving electron correlations[12,13] support the BR mechanisms proposed by the symmetry-stability analysis,[9] the thermochemical considerations[11] and experiments.[3]

Schuster et al.[14] proposed a chemically initiated electron-exchange luminescence (CIEEL) mechanism to account for the intense chemiluminescence in the decompositions of endoperoxides and dioxetanes. Their mechanism involves

CREST, Japan Science and Technology Corporation.

a complete one-electron transfer (ET), followed by annihilation of the generated radical ions. This process results in the generation of a excited singlet molecule, which emits the fluorescence (Chart 1).

On the other hand, White et al.[15] was the first to point out the important role of thermal change-transfer (CT) interactions in the decompositions of acylperoxy compounds (Chart 2). D denotes an electron donor, such as arylamine. CT complexes with strong one-electron-transfer (ET) BR characters instead of free ion-radical pairs could be activated complexes for the reactions, since the donor molecules employed in their studies were not very electron-rich. In fact, decomposition reactions require considerable activation energies, in contrast to the exothermic ion annihilations discussed by Bird et al.[16]

Dykstra et al.[17] have performed ab initio open-shell RHF 4-31G calculations on the radical anion of dioxetanone, and have shown that upon increasing the O–O bond distance (0.2 Å) from its equilibrium value, the energy of the radical anion of dioxetanone is dissociative, and irreversible cleavage follows immediately upon the receipt of an electron. As a result, they have concluded that the ab initio result is compatible with the CIEEL mechanism.[14,18–22] Since the calculations by Dykstra et al.[17] were limited to the less O–O elongated dioxetane, itself (R(OO) < 1.7 Å), we carried out the ab initio UHF calculations on the O–O dissociation reactions of anion radicals of dioxetane and dioxetanone.[23] First, the electron affinity of molecular oxygen, itself, was calculated using the 4-31G plus diffuse and 6-31G* basis sets. It was found that although the former basis set is more appropriate for the purpose than the latter, a correlation correction of about 1 eV is necessary for the former to reproduce the observed electron affinity of molecular oxygen. Therefore, by adding correlation corrections of 1 eV for the total energies of radical anions of dioxetane and dioxetanone, the potential curves of their decomposition reactions could be depicted, and the following conclusions were drawn:

(1) The calculated electron affinities (E_a) of both dioxetane and dioxetanone are negative at their equilibrium O–O lengths. However, the radical anions are largely stabilized by O–O elongation, leading to a large increase in the electron affinities. Obviously, the E_a-value of dioxetanone is larger than that of dioxetane.

(2) The intersection points between the potential curves for the neutral and radical anion forms are 15 kcal mol^{-1} for dioxetane and 11 kcal mol^{-1} for dioxetanone, respectively. These values could be close to the activation energies for the charge-transfer (CT) induced decompositions of these species.

UHF/4-31G plus diffuse calculations were also carried out to elucidate the endothermic electron-transfer reactions from the methyl anion to the O–O sigma bond of dioxetane and dioxetanone.[23] It was shown that a slight O–O elongation causes a drastic increase in the electron affinity of the peroxide bonds, followed by thermal ET from electron donors. Since extensive ab initio calculations were impossible in the cases of phenol, indole and luciferin anions at that time, we made semiempirical estimations of the one-electron transfer energies by the use of the ionization potentials determined by INDO calculations, together with the available experimental data.[23] The one ET was endothermic if the O–O bond of dioxetane was not elongated, though it indeed occurred after O–O elongation. From these theoretical results, we proposed the CT complex mechanism for chemiluminescence reactions. Namely, the electronic structure of an activated complex for the reactions was expressed by superposition of the ground and one ET configurations,[23]

$$\Phi(\mathrm{CT}) = C_0\Phi_0 + C_1\Phi_{\mathrm{ET}}, \quad (1)$$

where Φ_0 and Φ_{ET} denote, respectively, the no-ET and ET configurations. This CT mechanism involves two extreme cases: (1) $C_0 = 1$ and $C_1 = 0$, the homolytic dissociation,[1–3] and (2) $C_0 = 0$ and $C_1 = 1$, the complete one electron-transfer or CIEEL mechanism.[14] The ET BR character, given by $|C_1|^2$ for the complex, is approximately parallel to the magnitude of the CT excitation energy. Based on the calculated CT energies, the CT induced luminesence (CTIL) mechanism was presented for decomposition reactions with participation of electron-donor groups, as illustrated in Scheme 1. On experimental grounds, Catalani and Wilson[24] proposed a CT mechanism for chemiluminescence reactions, where the formation of a CT complex between vibrationally excited dioxetane and fluorescer was assumed to be the rate-determining step, resulting in a peroxide breakdown along with the simultaneous generation of some singlet fluorescener, directly from the transition state. Recently, several experimental

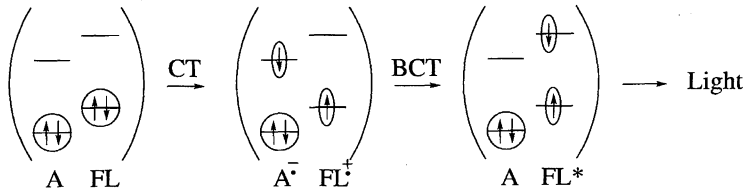

Chart 1.

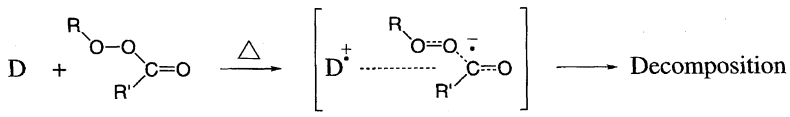

Chart 2.

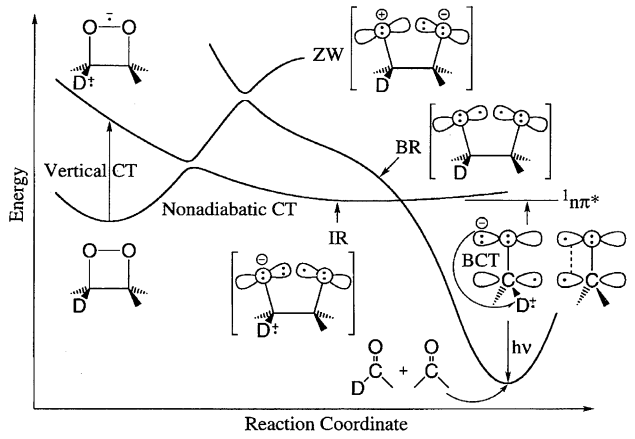

Scheme 1.

results[25—28] supported the CT mechanism[23] for chemiluminescence reactions.

In a previous paper,[29] we demonstrated an important role of the CT intermediates for oxygenation reactions between triplet molecular oxygen and the anionic species. The CT complex formation mechanism was successfully applied for base-catalyzed dioxygenations of phenol and indole derivatives. Many experimental results for the reaction systems by Nishinaga and co-workers[30] were consistent with the CT mechanism. In this succeeding study, post Hartree–Fock (HF) calculations of peroxyl radicals and ab initio HF MO calculations of phenol and indole anions were performed to re-examine the homolytic BR[9] and CT mechanisms[23] of the decomposition reactions of dioxetane and dioxetanones. The so-called even/odd relationships[31] for the efficiency of chemiluminescene reactions of the species were also examined on the basis of the ab initio results. The implications of the calculated results are discussed in relation to recent experimental results relating to the inter- and intramolecular CT-induced luminescence (CTIL) mechanism via the CT complex[23] and the CIEEL mechanism, assuming the generation of cation and anion radical fragments.[14]

1. Post Hartree–Fock Calculations of Electron Affinities of Oxygen Radicals

According to Benson and Nangia,[32] the electron affinities of oxygen radicals are 0.4—2.0 eV; for example, 0.44 (O_2), O (1.46), OH (1.83), OCH_3 (1.8) and O_2H (1.85). As mentioned above, HF calculations using of the 4-31G plus diffuse basis set provided the negative electron affinity of molecular oxygen, in contradiction to the experiment (E_a = 0.44 eV). In order to confirm previous theoretical treatments,[23] we first performed ab initio HF MO and post HF calculations to evaluate the electron affinities of oxygen radicals. UMP2 and RMP2/6-31G* energy-gradient calculations were, respectively, performed for the radical and anion states of the hydroxy (OH) and methoxy (OCH_3) species to obtain the optimized geometries. Assuming these geometries, the adiabatic electron affinities of these species were calculated using several extensive basis sets at the HF, MP2, and CCSD(T) levels. Table 1 summarizes the calculated results. From Table 1, the E_a-values of the OH group were negative at the HF level, even if large basis sets, such as the 6-311+G(3df,3pd) basis set, was used. The E_a-value was also negative at the CCSD(T)/6-311G** level. On the other hand, the experimental E_a-value (= 1.83 eV)[32] was qualitatively reproduced by MP2/6-311+G. These data show that both correlation corrections by the post HF methods and diffuse orbitals are necessary for computing the E_a-value of the OH radical. Similar situations were also recognized for the calculated electron affinities (E_a) of the methoxy group, for which the experimental value is 1.8 eV. The present calculated results support the previous semiempirical estimations of the electron affinities of the oxygen radicals.[23]

2. Decompositions of O–O Bonds of Neutral and Radical-Anion States

2.1. O–O Dissociation Process. In a previous examination,[23] as described in Introduction, a correlation correction of about 1.0 eV was necessary to qualitatively

Table 1. Adiabatic Electron Affinities (eV) of ·OH and ·OCH_3 Estimated at the Several Levels of Theories Using the Double Zeta and Their Extended Basis Sets

	·OH			·OCH_3		
Basis set	HF	MP2	CCSD(T)[a]	HF	MP2	CCSD(T)[a]
6-311G(d)	−1.34	−0.07	−0.25	−0.86	0.63	−0.47
6-311G(d,p)	−1.34	0.02	−0.17	−0.36	1.44	1.15
6-311+G	−0.17	1.53	1.31	−0.49	1.14	0.92
6-311++G	−0.17	1.53	1.31	−0.49	1.15	0.93
6-311++G(d)	−0.29	1.53	1.25	−0.35	1.37	1.07
6-311++G(d,p)	−0.25	1.64	1.35	−0.36	1.45	1.16
6-311++G(2d)	−0.31	1.69	1.37	−0.33	1.56	1.23
6-311++G(3d)	−0.30	1.81	1.50	−0.33	1.63	1.31
6-311++G(2d,p)	−0.27	1.77	1.45	−0.35	1.62	1.29
6-311++G(3d,p)	−0.27	1.87	1.56	−0.35	1.69	1.37
6-311+G(3df,3pd)	−0.28	1.94	1.63	−0.36	1.72	1.39
Exp.[b]			1.83			1.8±0.1

a) Geometies optimized at MP2 level were used. b) From Ref. 32.

reproduce the appropriate potential energies of decomposition reactions for the radical anions of dioxetane and dioxetanone. High-quality calculations for the electron affinities of hydroxyl and methoxyl radicals, such as shown in Table 1, indicate that the dynamical correlation corrections and the diffuse orbitals play important roles. It is, therefore, expected that the high-quality calculation gives the intersection points between the potential curves for the neutral and radical anion species in the O–O elongation during the early stage of the decomposition reaction of dioxetane and dioxetanone.

We carried out calculations of the potential curves of the O–O decomposition of hydrogen peroxide (HO–OH), which is the most simple case for the cleavage of the σ-bonding orbital in the O–O bond, and includes the essential behavior of O–O cleavage. The calculations were performed at the CCSD(T)/6-311++G(d) level. Figure 1 shows the potential curves of the neutral and radical anion of hydrogen peroxide (HO–OH). With O–O decomposition, the neutral state is rapidly destabilized, and the anion radical state is largely stabilized, leading the crossing point at 1.734 Å. The intersection point between two potential curves is higher by 15.1 kcal mol^{-1} than the neutral state, compared with 15 kcal mol^{-1} for dioxetane and 11 kcal mol^{-1} for dioxetanone,[23] respectively. These agreements insist that the addition of a correlation correction of 1.0 eV for the total energies calculated by the 4-31G plus diffuse is effective for studying the reaction mechanisms of chemiluminescence in the decompositions of dioxetane and dioxetanone derivatives.

2.2. Homolyses of Dioxetane. The closed-shell HF (RHF) solution was largely triplet-unstable for the O–O cleaved dioxetane,[9] being reorganized into DODS-type UHF MO's as follows:[9,10,33]

$$\Psi_{HO}^{\pm} = \cos\,\theta\sigma_{OO} \pm \sin\,\theta\sigma_{OO}^{*}, \qquad (2)$$

where σ_{OO} and σ_{OO}^{*} denote the bonding and antibonding O–O orbitals by the RHF approximation. The UHF MOs for the O–O cleaved dioxetane in Eq. 2 are essentially localized on the terminal oxygens, respectively. Therefore, there is one σ and one π radical center on each oxygen atom, and four BR configurations (σσ, σπ, πσ, ππ) are generated, as depicted in Fig. 2. The O–O cleavage of dioxetane is typical of a teratopic reaction in the sense of Turro and Devaquet.[34] From the orbital configurations shown in Fig. 2, the ^{1}σσ BR state is found to correlate with the ground (G) state of the fragments, while the ^{3}σσ BR state dissociates into the ^{3}ππ excited state. Thus, the state-correlation diagrams for all of the BR states are easily and qualitatively produced, as depicted in Fig. 2.[35]

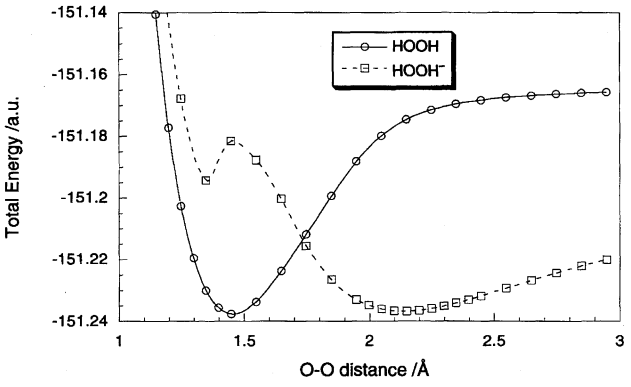

Fig. 1. Potential energy curves of the O–O decompositions for neutral and anion radical states of hydrogen peroxide (HO–OH) at the CCSD(T)/6-311++G(d) level.

Since the species about which we are presently concerned are rather large, we employed a qualitative procedure in order to elucidate possible mechanisms of chemiluminescence reactions. To this end, ab-initio UMP2/6-311+G(3d) calculations were carried out for the dioxetane and its O–O cleaved biradicals. Table 2 summarizes the relative energies and net charges for the O–O cleaved biradicals at r(OO) = 2.5 Å. From Table 2 the following energy-level ordering was concluded for the O–O cleaved biradicals:

$$^3\sigma\pi, ^3\pi\sigma < ^1\sigma\pi, ^1\pi\sigma < ^3\sigma\sigma < ^1\pi\pi < ^3\pi\pi < ^1\sigma\sigma. \qquad (3)$$

The energy difference between ^{3}σπ and ^{1}σσ is only 0.35 kcal mol^{-1}, compatible with the GVB/DZP results.[13] These ab-initio results, together with the orbital correlations given in Fig. 2, suggest a plausible reaction scheme for the thermolysis of dioxetane (DO), as follows:

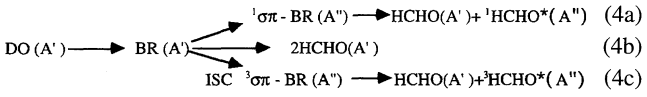

Probably, the ^{1}σσ and ^{3}σπ BR states are strongly spin-orbit

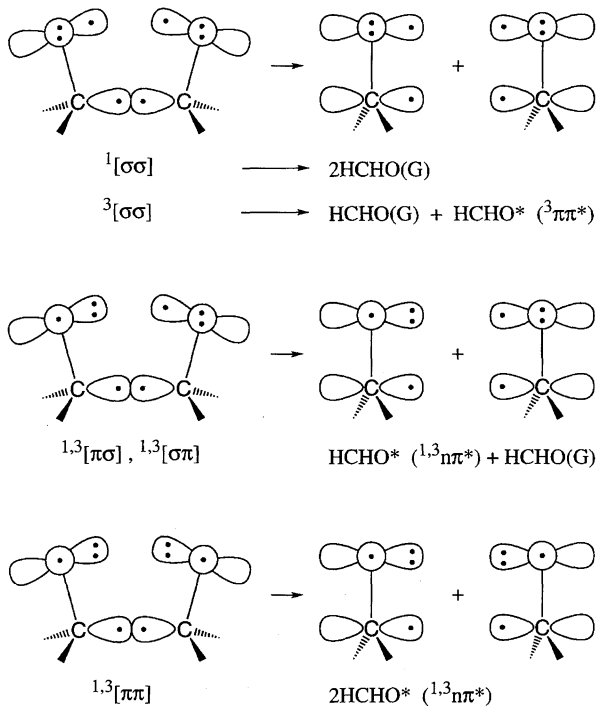

Fig. 2. Biradical (BR) configurations of the O–O elongation and correlations with the dissociation limits of two formaldehydes.

Table 2. Relative Energies (kcal mol^{-1}) and Net Charges for the Neutral and Anion Radical States of Dioxetane at Level of UMP2/6-311+G(3d)

	System[a,b]	E_{rel}	Net charges			
			C1	C2	O1	O2
DO	BR $^1[\sigma^1\sigma^1]$	0.0[c]	−0.09	−0.09	−0.55	−0.55
	$^1[\sigma^1\pi^1]$	−0.34	−0.12	−0.08	−0.52	−0.53
	$^1[\pi^1\pi^1]$	−0.31	−0.12	−0.12	−0.52	−0.52
	$^3[\sigma^1\sigma^1]$	−0.32	−0.08	−0.08	−0.54	−0.54
	$^3[\sigma^1\pi^1]$	−0.35	−0.12	−0.08	−0.52	−0.53
	$^3[\pi^1\pi^1]$	−0.29	−0.12	−0.12	−0.52	−0.52
DO^-	$^2[\sigma^2\sigma^1]$, $^2[\pi^2\sigma^1]$	0.0[d]	−0.08	−0.00	−0.53	−1.18
	$^2[\sigma^2\pi^1]$, $^2[\pi^2\pi^1]$	0.25	−0.14	−0.00	−0.52	−1.17

a) $^l[p^mq^n]$: l = spin multiplicity, and (m,n) = occupation number of p- and q- radical orbitals. b) O_1–O_2 bond distance is 2.5 Å. c) −227.7327 a.u. d) −227.7449 a.u.

coupled, because of their small energy gap, thus allowing intersystem crossing (ISC). Turro and Devaquet[34] suggested that the analogous $^1n\pi^*$ (A") to $^3\pi\pi^*$ (A') transition occurs with a rate constant of 10^{10} to 10^{11} s^{-1} for benzophenone. It is likely that the $^1\sigma\sigma$–$^3\sigma\pi$ BR transition possesses a comparative, or faster, rate. The fast ISC for $^1\sigma\sigma$–BR may indicate that the spin-forbidden pathway (4c) occurs in competition with, or even in preference to, the spin-allowed pathway (4a). The stepwise mechanism involving BR is compatible with recent detailed experiments on the thermolyses of dioxetanes.[36]

3. CT Induced Decompositions of Dioxetane and Dioxetanones

3.1. Methyl Anion Plus Dioxetane System. The ab-initio UHF calculations using the 4-31G+diffuse basis set were carried out to elucidate the endothermic CT reactions from electron donors (D) to the OO bond of peroxides. To this end, the methyl anion (**1**) plus dioxetane system was examined, as shown in Fig. 3, where variable R denotes the intermolecular distance between the carbon anion and the center of the O–O bond of dioxetane; r means the O–O bond distance. Table 3 summarizes the obtained relative energies and net charges. Figure 4 shows the potential surface of the obtained system. From Fig. 4, the O–O bond elongation, i.e., O–O vibration, causes a drastic increase in its electron affinity, accompanied by a thermal CT reaction from the methyl anion to the O–O bond, even at a relatively large intermolecular distance ($R > 4.0$ Å). This process is more favorable than the other process, which would involve a CT at a relatively small R without O–O elongation, followed by a subsequent O–O cleavage reaction of the anion radical. The endothermicity for the former process arises from the activation energy, which is necessary for the slight O–O elongation, whereas the activation barrier for the latter process is responsible for the ET process, itself; one ET is energetically unfavorable for dioxetane at the equilibrium geometry, because of a large negative electron affinity. The ab-initio MO results given

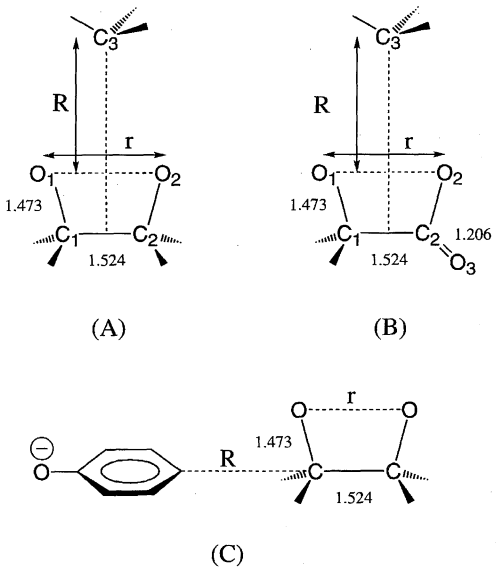

Fig. 3. Molecular structures of methyl anion (**1**) plus dioxetane (A) and dioxetanone (B) and phenoxide anion (**III**) plus dioxetane (C) systems. R and r means variables for the O–O cleavage reaction of these systems.

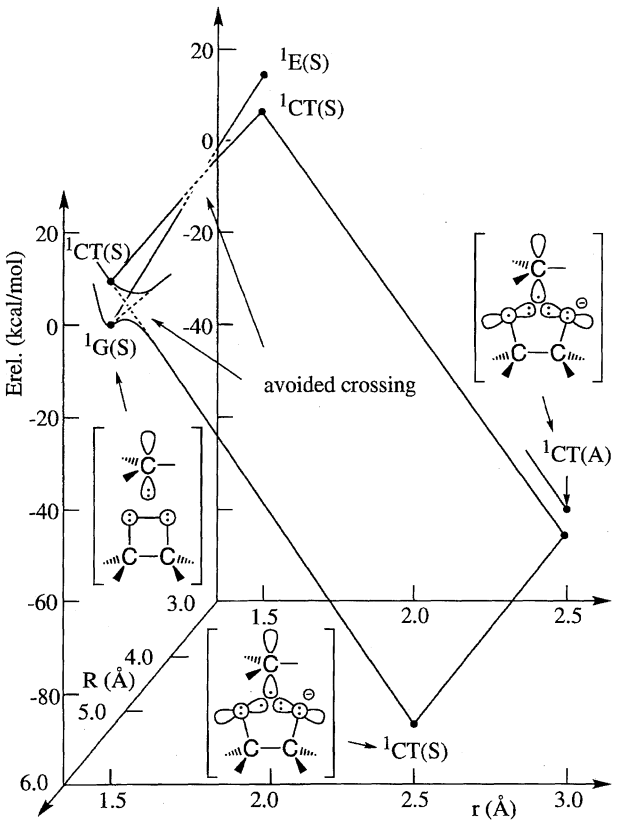

Fig. 4. Potential surface for the O–O cleavage reaction of dioxetane assisted by the charge-transfer (CT) from methyl anion to the O–O σ^* orbital.

in Table 3 are compatible with the O–O elongation mechanism followed by the CT complex formation reaction, which is the essence of our endothermic CT mechanism[23] for the chemiluminescence reaction of dioxetane. However, the en-

Table 3. Relative Energies and Net Charges of the Dioxetane (Dioxetanone) Plus Methyl Anion and Dioxetane (Dioxetanone) Anion Plus Methyl Radical Systems by Ab-Initio UHF Method[a)]

System	R	r	E_{rel}	Net charges					
				C1	C2	O1	O2	C3	(O)
DO+CH_3^-	3.0	1.497	15.6	−0.47	−0.47	0.00	0.00	−1.33	
	6.0	1.497	0.0[b)]	−0.37	−0.37	−0.09	−0.09	−1.23	
DO AN$^{\cdot-}$[σ^1]+·CH_3[σ^1]	3.0	1.497	7.47	−0.46	−0.46	−0.24	−0.24	−0.61	
	6.0	1.497	7.27	−0.42	−0.42	−0.33	−0.37	−0.51	
	3.0	2.5	−87.7	−0.39	−0.37	−0.06	−0.70	−0.54	
	4.0	2.5	−88.1	−0.38	−0.36	−0.09	−0.73	−0.50	
	5.0	2.5	−88.2	−0.37	−0.35	−0.10	−0.74	−0.50	
	6.0	2.5	−88.3	−0.37	−0.35	−0.11	−0.75	−0.51	
DO AN$^{\cdot-}$[π^1]+·CH_3[σ^1]	3.0	2.5	−81.5	−0.43	−0.38	−0.05	−0.69	−0.54	
DON+CH_3^-	3.0	1.497	9.74	−0.52	0.33	0.18	0.14	−1.39	−0.47
	6.0	1.497	0.0[c)]	−0.40	0.41	−0.04	−0.06	−1.23	−0.42
DON AN$^{\cdot-}$[σ^1]+·CH_3[σ^1]	3.0	2.5	−109	−0.48	0.24	−0.04	−0.56	−0.56	−0.51
	6.0	2.5	−109	−0.46	0.26	−0.09	−0.62	−0.52	−0.50

a) 4-31G plus diffuse basis set. b) −266.7310 a.u. c) −340.3364 a.u.

dothermic activation barrier is almost negligible, showing that the CTIL mechanism[23)] is essentially regarded as being a CIEEL type[14)] in this case; the coefficient C_1 is very large in Eq. 1. This is compatible with the conclusion obtained by Dykstra et al.[17)]

The ab-initio UHF calculations by 4-31G plus diffuse basis set were carried out for several geometries of the methyl anion (**1**) plus dioxetanone system illustrated in Fig. 3. Table 3 gives the relative energies and net charges for the intermediates formed before and after CT from the methyl anion to the O–O bond. From Table 3, the CTIL mechanism, which is almost equivalent to the one ET mechanism in this case, should be operative for the CT induced decompositions of dioxetanone by the methyl anion. The situations are quite similar in the case of the Russell mechanism of reactions between triplet molecular oxygen and carbanions (**2**), as previously examined.[29)]

3.2. Phenoxide Anion Plus Dioxetane System. It has been reported that the dioxetane derivatives substituted by the electron-donating groups have high quantum yields of the chemiluminescence reactions.[19b)] The phenoxide anion (**3**) plus dioxetane system shown in Fig. 3(C) was calculated at the UHF/4-31G level, and the atomic charge densities of the dioxetane moiety are shown in Fig. 5. The total charge density of the dioxetane moiety is given by −0.039 for the case of the phenoxide monoanion, showing a small charge transfer from the phenoxide monoanion as an electron donor. On the contrary, the charge density of the dioxetane moiety is increased to −0.063 by a charge transfer from the phenoxide dianion. The electron transfer is rather small because of the near orthogonality between the donor and acceptor MOs. This indicates that an encounter with an electron-rich molecule, which has high possibilities of donating electrons, induces a charge transfer to lead the CT complex, if the symmetry requirement for orbital interaction is satisfied. The present calculations are consistent with the CT mechanism suggested by Catalani and Wilson[24)] as well as others.[25—28)]

3.3. CT Induced Decomposition. The above-mentioned ab-initio MO calculations indicate that the thermal CT reaction from anionic species to the O–O elongated dioxetane is a key step for the chemiluminescence reactions of dioxetane and dioxetanone. The electronic structure of the activated complex for the reactions could be expressed by a superposition of the ground and one ET configurations, whose energies are sensitive to solution. Then, Eq. 1 in the introduction can be rewritten as

$$\Phi(\mathrm{CT})_{\mathrm{solv}} = C_0(\mathrm{solv})\Phi_0 + C_1(\mathrm{solv})\Phi_{\mathrm{ET}}, \quad (5)$$

where Φ_0 and Φ_{ET} denote, respectively, the no-ET and one-ET configurations. The stabilization energy (E_{total}) and the CT excitation energy (ΔE_{CT}) are given as the functions of

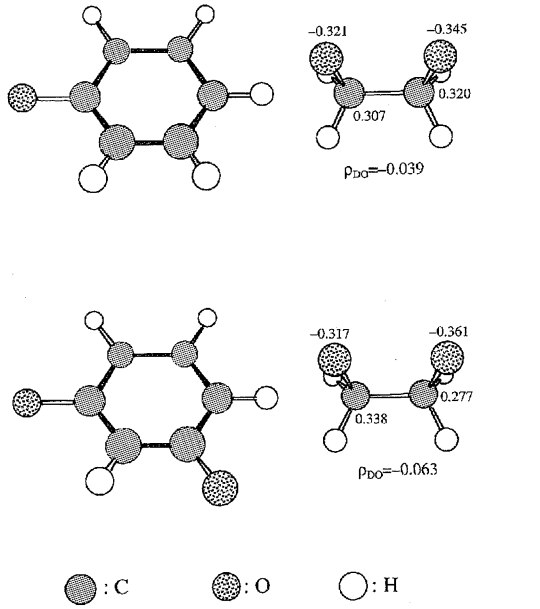

Fig. 5. Atomic densities of dioxetane moiety in phenoxide anion (**III**) plus dioxetane system. Distance between the nearest carbon atoms in benzene and dioxetane rings is 3.0 Å and O–O distance in dioxetane moiety is 2.5 Å.

$(\gamma+E_S)$, as follows:

$$E^{\pm} = \frac{1}{2}\{(\gamma+E_S) \pm \sqrt{(\gamma+E_S)^2+4W^2}\}, \quad (6)$$

$$\Delta E_{CT} = \sqrt{(\gamma+E_S)^2+4W^2}, \quad (7)$$

where E_S is the solvation energy difference between the no-ET and one-ET configurations. γ is the energy difference between these configurations, and is approximately given by

$$\gamma = I_p - E_a + J_{AD}. \quad (8)$$

I_p and E_a are the ionization potential of the donor and electron affinity of dioxetane (DO), respectively. J_{AD} is the Coulombic attraction between the radical pairs [D·DO$^-$]. W is the interaction term between the two configurations, and is proportional to the orbital overlap (S) between the O–O sigma antibonding orbital and HOMO of electron donor (D),

$$W = < \Phi_0|H|\Phi_{ET} > = \text{const} \times S(\sigma^*(OO)/HOMO(D)). \quad (9)$$

The stabilization energy (E_{total}) becomes larger if the solvation energy (E_S) is large and the γ-value is small. For a large E_S and small γ, E_{total} may well become large enough to outweigh the exchange repulsion energy. As a consequence, an intermediate with a strong CT character may be formed. The CT character (X_{CT}) is defined with the weight of the ET configuration in Eq. 5 as follows:

$$X_{CT} = C_1^2, \quad (10)$$

where the complete one ET BR (namely CIEEL) corresponds to one of the extreme ($X_{CT} = 1$), while the homolysis corresponds to the other extreme ($X_{CT} = 0$). The functional dependences of E_{total}, ΔE_{CT}, and X_{CT} on $(\gamma+E_S)$ have already been depicted in Figs.10 and 11 of Ref. 29. Fig. 11 of Ref. 29 is reproduced here as Fig. 6 in order to aid understanding of our discussion.

From Fig. 6, a positive value of $(\gamma+E_S)$, which represents that the ground configuration is more stable than the ET configurations, provides a X_{CT} value of less than 50%, while a negative value gives a X_{CT} value of more than 50%. These relationships in Fig. 6 can be used to estimate the ET character for an activation complex, namely the CT complex. The ground configuration is more stable than the ET configuration at a relatively longer intermolecular distance, whereas

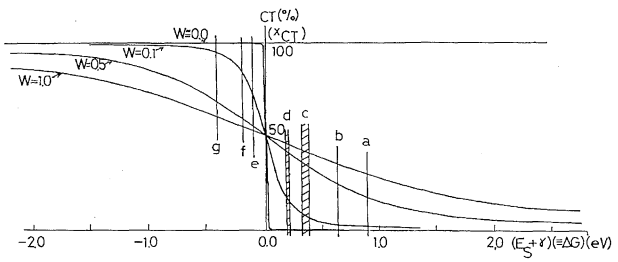

Fig. 6. Variations of the calculated CT characters against the CT energy, $\gamma+E_s$. This figure is reproduced from Fig.11 of Ref. 29 with permission. The notations (a)—(g) are described in Fig. 10 of Ref. 29.

is sharply destabilized at a shorter distance, because of the exchange repulsion. On the other hand, the ET configuration is stabilized at an early stage, becoming more stable than the ground configuration. Therefore, the avoided crossing between the Φ_0 and Φ_{ET} configurations occurs, as shown in Scheme 1. This leads to the formation of the CT complex with a strong CT character on the ground-state surface. In fact, as can be seen from Table 2 and Fig. 4, the charges transfer from the donar to DO. Thus, the reaction of the phenoxide anion with dioxetane proceeds through the CT mechanism in solution.

3.4. Estimations of CT Characters in Gas and Nonpolar Solution. Figure 6 shows that the weight (X_{CT}) of the ET configuration is essentially determined by the energy gap between the ground and ET configurations, which are parallel to the ionization potential (I_p) of donor anion, as shown in Eq. 7. Unfortunately, the gas-phase I_p's of monoanions of phenol (**3**) and indole (**4**) derivatives have not yet been reported, although those of their neutral forms have been determined by UPS experiments by Houk et al.[37] and others.[38,39] Therefore, the I_p's of various phenol and indole derivatives were calculated using the INDO method under the assumption $I_p = -\beta\varepsilon_{HO}$, where ε_{HO} means the orbital energy of the HOMO. The coefficient β (-0.762) was determined to reproduce the observed I_p's within ± 0.3 eV. The calculated I_p values are already given in Tables 5 and 6 of the Ref. 29.

Table 4 summarizes the empirically corrected and ab initio estimations of the ionization potentials, assuming Koopman's theorem, of phenol derivatives together with the observed vertical I_p's. It can be seen from Table 4 that the ab initio and empirical I_p values well reproduce the observed values. This indicates that qualitative estimations by INDO are available for studying the CT mechanism for the decomposition of dioxetane, dioxetanone, and so on.

The I_p's of phenol derivatives are reduced by about 6.2 eV along with the deprotonation of OH. Therefore, deprotonations of the species catalyzed by bases lead to a paramount increase in their reactivities to dioxetane. This implies that deprotonation of the OH group in the phenol derivatives could be a trigger to induce CT decomposition mechanisms of dioxetanes, in accord with several experiments.[22—28]

The monoanions of substituted phenols and indoles are often electron donors in the case of synthetic model compounds for luciferins, which are known to be substrates related to bioluminescences.[4] Here, the model compounds for firefly (**5**), cypiridina (**6**), and coelenterate (**7**) luciferins were

Table 4. Ionization Potentials I_p (eV) of Phenol, Indole, and Their Monoanion Assuming Koopmans Theorem

Compounds	RHF/6-311+G	INDO[a]	Exp.
Phenol	8.74	8.85	8.74[b]
Phenol anion	2.58	1.57	
Indole		7.91	7.92[c]
Indole anion		2.01	

a) Ref. 29. b) Ref. 37. c) Ref. 39.

Table 5. Ionization Potentials I_p and CT Exitation Energies to Dioxetanone, and Activation Energies $E^{\neq}$ and Mechanisms of the Chemiluminescence Reactions for Model Compounds for Luciferin Derivatives. Values are Given in Unit of eV

System	R_1	R_2	I_p [a)]	γ [a)]	$E^{\neq}$ [b)]	M.C.[c)]
5$_a$	CH	H	5.40	2.40	1.46	BR
5$_b$	C^-	H	1.27	1.27	0.77	CT
6$_a$	CH	NH	6.12	3.12	1.90	BR
6$_b$	C^-	NH	0.45	0.45	0.27	CT
6$_c$	CH	N^-	1.25	1.25	0.76	CT
6$_d$	C^-	N^-	−0.83	−0.83	−0.51	CIEEL
7$_a$	CH	OH	6.27	3.27	1.99	BR
7$_b$	C^-	OH	0.50	0.50	0.31	CT

a) see Eq. 8, where J_{AD} is 0.0 for the mono- and di-anion systems and 3.0 (eV) for the system without formal charge. b) Eq. 11. c) BR = homolysis via BR, CT = endothermic decomposition induced by CT, and CIEEL = one electron-transfer (ET) biradical mechanism.

examined, as illustrated in Fig. 7. The I_p's of these species were calculated by previously described procedures.[29] Table 5 summarizes the obtained ionization potentials (I_p). The I_p's of neutral luciferins **5**—**7** were calculated to be smaller by about 1.8—2.3 eV than those of the indole derivatives. Similarly, the monoanions of the luciferin models have lower I_p's than those of phenol and indole.

The calculated I_p's of monoanions of phenol, indole, and luciferins were used to estimate the CT excitation energies (γ) for the O–O bond (E_a = 0.0 eV) of dioxetanone and the O-radical site (E_a = 1.68 eV) of the O–O cleaved dioxetanone. State-correlation diagrams for the O–O cleavage reaction are depicted in Fig. 8 based on the resulting CT energies. From Fig. 8, we see that the vertical CT state is less stable than the nonvertical CT state, in accord with the ab-initio surface in Fig. 4. The CT-induced O–O dissociations are, therefore, endothermic, indicating that a slight O–O elongation is crucial at the transition state. The activation energies ($E^{\#}$) are calculated using the I_p's of the electron donors in the model calculations,

$$E^{\#}(\mathrm{CT}) = 0.61 I_p(\gamma). \quad (11)$$

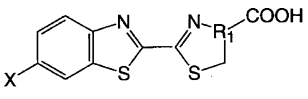

5

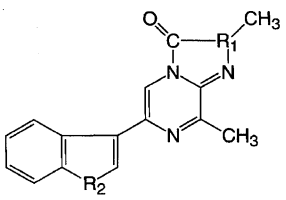

6

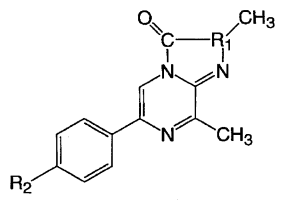

7

Fig. 7. Molecular structures of firefly (**V**), cypiridina (**VI**), and corenterate (**VII**) luciferins.

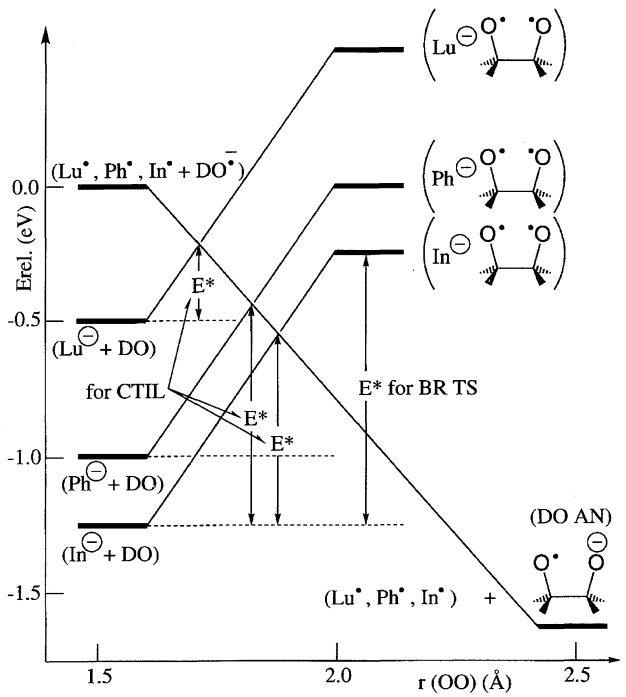

Fig. 8. State correlation diagrams for the decomposition reaction of dioxetane induced by the charge transfer from luciferine (Lu), phenol (Ph), and indole (In) monoanions to the O–O σ^* orbital

where I_p should be replaced by the vertical CT energy (γ) in the case of neutral systems, for which the Coulombic energy (J_{AD}) is not negligible. From Eq. 11, the BR mechanism via the O–O homolysis should be more favorable than the CT complex formation mechanism via the endothermic CT if I_p (γ) exceeds a threshold value. The reaction mechanisms for luciferin derivatives (**5**—**7**) are also summarized in Table 5.

4. Possible Mechanisms of Generations of Excited States

4.1. Decompositions of Anion Radicals of Dioxetane. Let us consider the state-correlation diagram for the C–C cleavage reactions of the dioxetane anion radicals in order to elucidate the possible mechanisms of chemiluminescence reactions. For this purpose, the state correlations for the dioxetane anion radical, itself, were considered. Although the O–O sigma antibonding orbital accepts one electron at the equilibrium geometry of dioxetane, four different BR configurations at the O–O cleaved geometry can accept the electron, affording anion radicals with the $(\sigma^2\sigma^1) = (\sigma^1\pi^2)$ and $(\sigma^2\pi^1) = (\pi^2\pi^1)$ configurations. The ab initio UMP2/6-311+G calculations were carried out for anion radicals of its O–O cleaved biradicals. Table 2 summarizes the relative energies and net charges for the O–O cleaved anion radicals at r(OO) = 2.5 Å. From Table 2 the following energy-level ordering was concluded for the O–O cleaved anion radicals:

$$(\sigma^2\sigma^1) = (\sigma^1\pi^2) < (\sigma^2\pi^1) = (\pi^2\pi^1). \quad (12)$$

The energy difference between $(\sigma^2\sigma^1)$ and $(\pi^2\pi^1)$ is only 0.25 kcal mol^{-1}. These ab initio results shown in Fig. 9

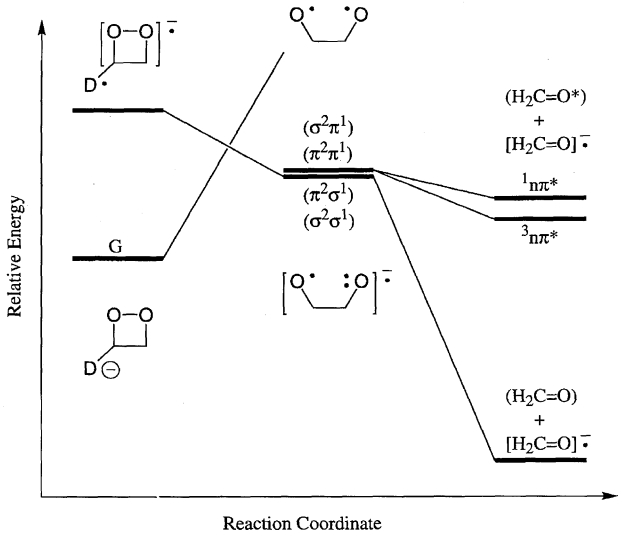

Fig. 9. The state correlation diagram of the decomposition of the anion radical of dioxetane.

suggest possible reaction schemes for the decomposition of the dioxetane anion radical: (1) the $\sigma^2\sigma^1$ and $\sigma^1\pi^2$ anion radicals decompose into the ground states of the π^*-anion radical of HCHO and neutral HCHO and (2) the $\sigma^2\pi^1$ and $\pi^2\pi^1$ anion radicals provide ground states of the π-anion radical of HCHO and a singlet or triplet $n\pi^*$ excited state of neutral HCHO.

4.2. Transition State Model for Chemiluminescence Reactions. Extensive ab initio energy-gradient calculations are necessary to determine the locations of the transition structures in the back CT (BCT) region in Scheme 1. Such calculations are hardly accomplished for dioxetane radical anions with large electron-donating groups. Therefore, we present here a qualitative configuration interaction (CI) model for the BCT process. Since three potential curves are nearly degenerate in energy in the BCT region in Scheme 1, the electronic structure of the BCT complex can be expressed by the superpositions of three configurations, as

$$\begin{aligned}\Phi(\mathrm{BCT}) = {} & d_0\,\Phi_{\mathrm{ET}}(\mathrm{D^+{-}[CH{=}O]^-/H_2C{=}O}) \\ & + d_1\,\Phi_{\mathrm{LE}}(\mathrm{D^*{-}CH{=}O/H_2C{=}O}) \\ & + d_2\,\Phi_{\mathrm{G}}(\mathrm{D{-}CH{=}O/H_2C{=}O}),\end{aligned} \tag{13}$$

where Φ_{ET}, Φ_{LE}, and Φ_{G} denote, respectively, the one ET, locally excited, and ground configurations. The mixing coefficients (d_1 and d_2) are determined by the interaction matrix elements, which are approximately given by the orbital overlap (S), as follows:

$$d_1 \propto W_1 = \langle \Phi_{\mathrm{ET}}|\mathrm{H}|\Phi_{\mathrm{LE}}\rangle = \text{const.} \times S(\pi^*(\mathrm{C{=}O})/\mathrm{LUMO\ (D)}), \tag{14a}$$

$$d_2 \propto W_2 = \langle \Phi_{\mathrm{ET}}|\mathrm{H}|\Phi_{\mathrm{G}}\rangle = \text{const.} \times S(\pi^*(\mathrm{C{=}O})/\mathrm{HOMO\ (D)}). \tag{14b}$$

Then, the HOMO and LUMO of the carbonyl compounds (D–CH=O) should in turn be given by

$$\mathrm{HOMO\ (D{-}CH{=}O)} = \mathrm{HOMO\ (D)} + \delta\pi^*\ (\mathrm{C{=}O}), \tag{15a}$$

$$\mathrm{LUMO\ (D{-}CH{=}O)} = \mathrm{LUMO\ (D)} + \delta\pi^*\ (\mathrm{C{=}O}). \tag{15b}$$

The orbital-symmetry rules are applicable to predict the magnitude of the mixing coefficients (d_1 and d_2), as illustrated in Fig. 10. In the case of A in Fig. 10, the π^*-MO of the carbonyl group is approximately regarded as being symmetric (S) with respect to the σ_v plane, and the LUMO of the donor also has S-symmetry. The excited state is preferentially generated from an interaction of those two orbitals, as shown in A of Fig. 10, affording chemiluminescence efficiently. On the other hand, the CT complex easily collapses into the ground state if the HOMO of the donor is symmetric (S), as illustrated by B in Fig. 10. The efficiency of chemiluminescence should be low in this case. The selection rules for chemiluminescence reactions are thus derived based on the CT complex model for the BCT process given by Eq. 13.

4.3. The Odd/Even Selection Rule for Chemiluminescence. Several experimental results have clarified the odd/even selection rules for the efficiency of the chemiluminescence reactions of dioxetane derivatives with phenoxide anion groups. The chemiluminescence yield is usually high for meta-substituted phenoxide species, while it is low for para-substituted ones. McCapra explained these differences on the basis of his concerted decomposition mechanism of dioxetanes. Here, the odd/even selection rules are alternately explained by our CT complex mechanism, expressed by Eq. 13.

Let's consider the CT complex of carbonyl compounds substituted by *para-* and *meta*-phenoxide anion radicals, as shown in Fig. 11. In the case of the *p*-phenoxide anion radical, corresponding to (A) and (B) in Fig. 11, the π^*-orbital of the carbonyl group interacts with HOMO of the phenoxy radical, while the overlap between the π^*-orbital of the carbonyl group and LUMO of the phenoxy radical is negligible, due to the orbital symmetries. This indicates that the *para*-substituted phenoxy radical causes an easy collapse of the CT complex into the ground state in the back CT region. On the contrary, the behaviors of the *meta*-substitution are reversed. The π^*-orbital of the carbonyl group predominantly interacts

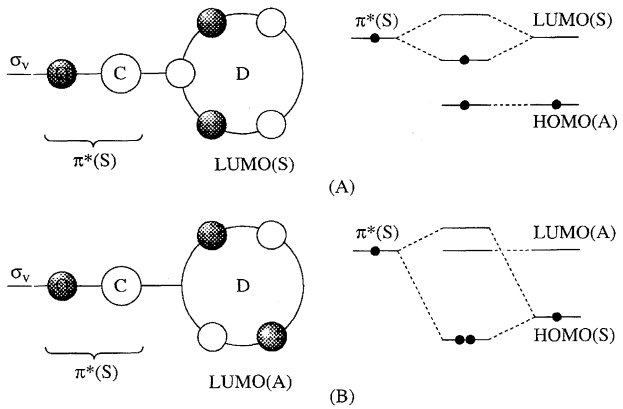

Fig. 10. Schematic presentation of the interaction of the carbonyl moiety and the donar: (A) presents the case of mixing coefficient d_1 and (B) presents the case of mixing coefficient d_2.

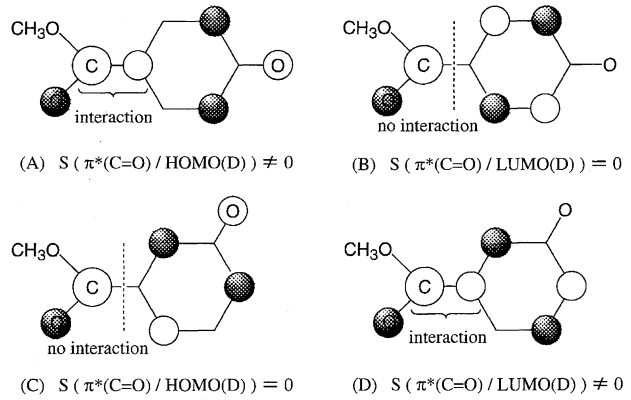

Fig. 11. Schematic presentation of the odd/even selection rule for chemiluminescence.

with the LUMO of the meta-substituted phenoxy radical, increasing the mixing between configurations of Φ_{ET} and Φ_{LE} in Eq. 14a. This process in the BCT region enhances the chemiluminescence efficiency. These considerations, based on the interactions of the electron configurations and/or orbital mixing, correspond to the odd/even selection rules for the efficiency of the chemiluminescence reactions of dioxetane derivatives with phenoxide anion groups.

In order to confirm the our consideration for the odd/even selection rule, the ground state of the *m*-hydroxyphenyl methyl ketone, which corresponds to the product of the thermal decomposition of dioxetane, was calculated at the RHF/6-31+G level. The HOMO and second LUMO are drawn in Fig. 12. It can be easily seen from Fig. 12 that the HOMO, which is a π-orbital localized on a *m*-hydroxyphenyl substituent, dose not interact with the π*-orbital of the carbonyl group, while the second LUMO has a strong bonding character between the LUMO of the phenol and π*-orbital of the carbonyl group. These behaviors of MOs coincide with the case of (C) and (D), schematically shown in Fig. 11. The *meta*-substituted phenol induces the BCT due to mixing between configurations of Φ_{ET} and Φ_{LE} according to Eq. 14a,

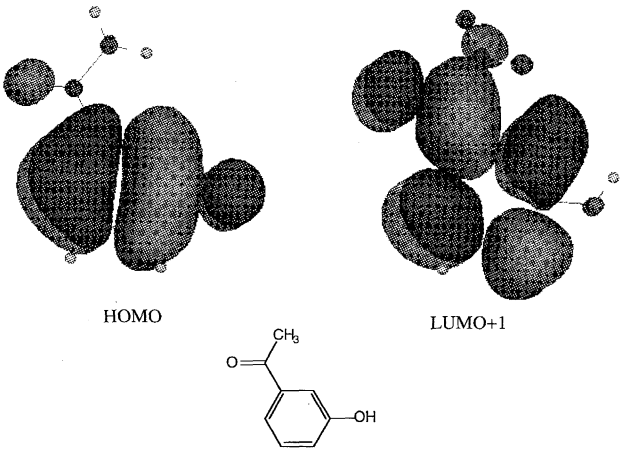

Fig. 12. Highest occupied molecular orbital (HOMO) and second lowest unoccupied molecular orbital (LUMO+1) of *m*-hydroxyphenyl methyl ketone calculated at RHF/6-31+G level.

leading to a high chemiluminescence yield.

5. Discussions and Concluding Remarks

The CIEEL process for the luminescence reactions by Schuster et al.[14] is formally regarded as being an annihilation of generated thermally radical ions.[16,40] However, the vertical CT excitations from an electron-donating groups, such as phenol, indole, and arylamines to the O–O bonds of dioxetane and dioxetanone groups, are more or less endothermic in less-polar solvents, as depicted in Scheme 1. Obviously, the vertical CT excitation energies cannot explain the experimentally determined low activation energies of the chemiluminescence reactions, which are about 13—20 kcal mol^{-1}. The CT step induced by O–O elongation is thus regarded as being the rate-determining endothermic process in the decomposition reactions of dioxetanes. Therefore, the electronic structure of the activated complexes is described by the superposition of the ground and CT configurations,[23] instead of the complete one-ET structure.[14] Therefore, we have referred to these reactions as being CT induced chemiluminescence reactions (CTIL).[23] The present theoretical calculations indicate that the CT complex formations should be operative for CTIL, in accord with the CT mechanism by Catalani and Wilson,[24] and recent experimental results by others.[25—28]

The ab initio model calculations on the methyl anion plus dioxetane system lend support to the so-called CT mechanism for the chemiluminescence reactions.[24—29] Here, some important aspects are discussed based on the calculated results. McCapra[18a] as well as Schuster and his collaborators[14] have shown that the intra-molecular one ET plays a crucial role in the chemiluminescence of firefly luciferin. They have considered that the one ET from the donor part (X = O^-) to the dioxetanone skeleton is the primary step of this reaction (Chart 3). The back CT (BCT) from the released CO_2^- to the remaining carbonyl group generates an excited singlet state, which exhibits the luminescence. On the other hand, the chemiluminescence was largely reduced when the X (= O^-) in firefly luciferin was replaced by OMe and OH. This implies that a strong electron-donating group is necessary for the CIEEL process. In fact, the CT excitation energy become over 1.7 eV for firefly luciferins without an anionic site, as shown in Table 5. Then, the O–O homolysis could be predominant over the CT-induced decomposition in the latter case.

Schaap et al.[19,25] have investigated the thermal decomposition of dioxetanes **8** and **9** with electron-rich aromatic groups, as shown in Fig. 13, and have shown that the CT

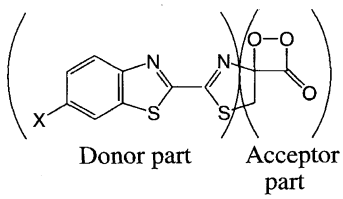

Chart 3.

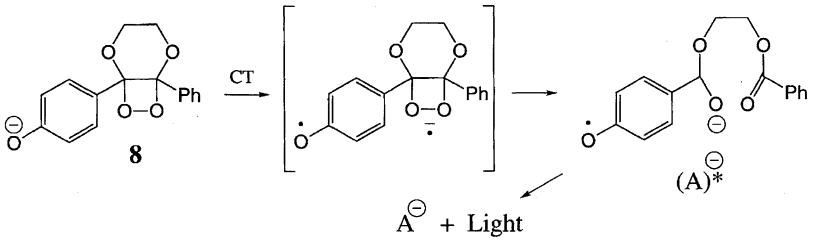

Chart 4.

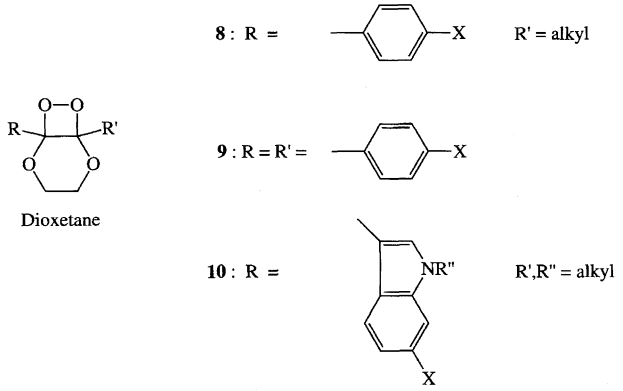

Fig. 13. Molecular structures of electron-rich dioxetanes.

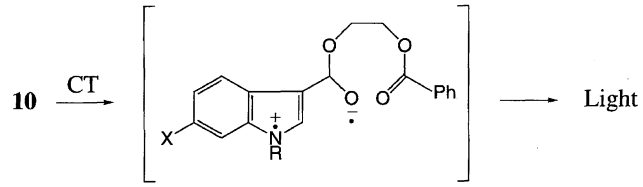

Chart 5.

mechanism is certainly operative for the decomposition of **9** with X = O^-, whereas the homopolar biradical (BR) mechanism is more reasonable for **8** with X = OH (Chart 4). They have suggested that the direct emission stems from the anion radical generated by the thermal intramolecular CT from the phenoxide anion group to the σ^*_{OO} bond. Their results imply that the excited singlet state arises directly from the CT complex, which is regarded as being the transition state. Schaap et al.[19] have reported that the CT mechanism is operative for **9** with X = $N(Me)_2$, whereas the biradical pathway is more appropriate for **9** with X = OMe, OH, and Cl_3. Schaap et al.[25] also reported CT-induced chemiluminescence reactions of dioxetanes with the adamantane group; the yield of the excited state is very high (> 50%) in this case.

Goto and co-worker[21] have also investigated the decompositions of dioxetanes with indol groups (**10**), and have concluded that the decomposition mechanism is converted from homolysis to CT induced decomposition along with an increase in the electron-donating ability of substituent X (Chart 5). They first observed the luminescence from the exciplex with the CT character (see. Eq. 4). Since **9** and **10** can be regarded as being models of the dioxetanes of cypridina and colenterate luciferins, respectively, the CTIL mechanisms are probably applicable to the bioluminescence reactions of these luciferins, since deprotonation of the phenol or indole group of luciferins is highly effective for increasing the electron-pushing ability.

Matsumoto and co-workers[27] synthesized many dioxetane derivatives, and investigated the substituent effects on the chemiluminescence of dioxetanes substituted by the *meta*-phenoxy derivatives. They found that the orbital interactions and conformations between the phenoxide anion and the dioxetane ring play important roles concerning chemiluminescence efficiency. These experimental results are consistent with our theoretical study on the mechanism of thermal decomposition of the dioxetane derivatives, supporting the CTIL mechanisms.

Kimura et al.[28] found a bell-shape correlation curve for a plot of the Hammett σ constant and the quantum yields of the formation of excited amidines from the chemiluminescent reaction of 2-(*p*-dimethylaminophenyl)-4,5-bis(*p*-X-phenyl)-4-hydroperoxy-4*H*-imidazoles (**11**) (X = OCH_3, H, F, Cl, CF_3, and CN) (Chart 6). They reported that the *p*-fluorine-substituted species is the most efficient member of **11**, exhibiting a high quantum yield of fluorenscence (0.79), which is comparable to that of firefly bioluminescence. They also pointed out that the excited state is generated from an exothermic ET step, because of the existence of an inversion region predicted by Marcus,[41] which is in compatible with the CT mechanism by Catalani and Wilson[24] and others.[25—28] Our energy diagram in Fig. 14 is also consistent with the experimental results.[28]

The electron affinity of the O–O anti-bonding orbital increases along with an increase in the O–O distance R(O–O) : $E_a = dR$(O–O) (where d is constant). Therefore, the CT excitation energy (γ) from the anionic site to the O–O bond decreases along with O–O elongation. Figure 14 illustrates the potential curves of the no-ET and ET configurations against the O–O distance. From Fig. 14, there are three curve crossing regions, depending on the ioniza-

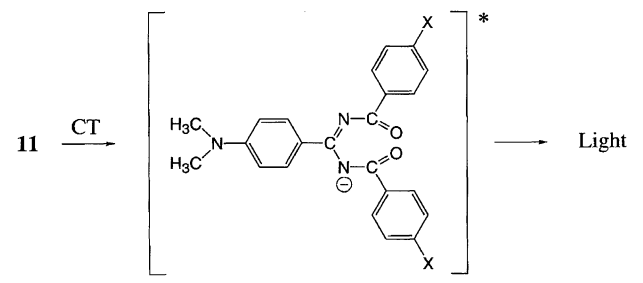

Chart 6.

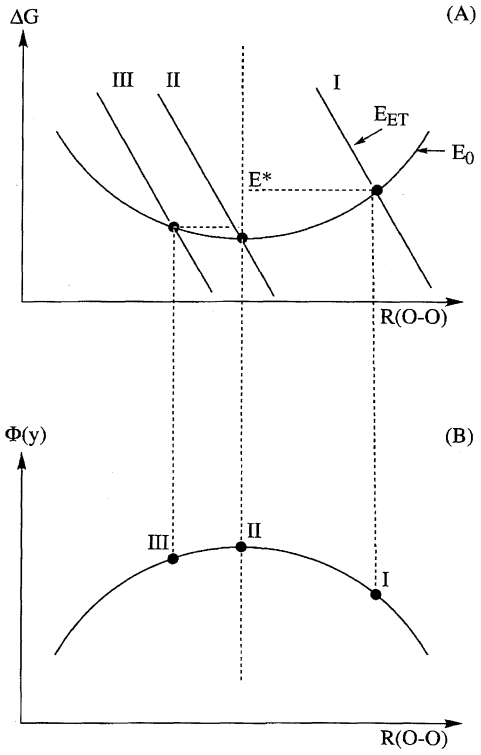

Fig. 14. Schematic illustration of the potential curves of the no ET and ET configurations against the O–O distance.

tion potentials (or oxidation potentials) of anionic groups: I; normal, II; maximum ($E_a = 0$), and III; inversion regions. The bell-shaped dependence of the yield of fluorenscer is expected, as illustrated in Fig. 14, because the rate of ET should be maximum in case II. This is consistent with recent experimental results by Kimura et al.[28]

Kemal and Bruice[42] have reported model reactions of dihydroflavin FMNH2 with aldehyde to provide bioluminescences. The reaction scheme derived from their results could involve intramolecular CT from the FMNH to the O–O bond as a key step. Their CT reaction seems to be energetically accessible from the low I_p's of FMNH (see Table 9 in Ref. 29), although it is slightly endothernic. The luminescence reaction could be a model of the bioluminescence reactions of carbonyl groups catalyzed by flavin enzymes.

This work was supported by CREST (Core Research for Evolutional Science and Technology) of Japan Science and Technology Corporation (JST) and by Grant-in-Aid for Science Research on Priority Areas (No. 283, "Inovative Synthetic Reactions") from the Ministry of Education, Science, Sports and Culture.

References

1) F. McCapra, *Q. Rev. Chem. Soc.*, **1966**, 485.
2) T. Wilson, *Int. Rev. Sci.: Phys. Chem. Ser. 2.*, **9**, 265 (1976).
3) W. Adam, *Pure Appl. Chem.*, **52**, 2591(1980).
4) A. Mayer and S. Neuenhofer, *Angew. Chem., Int. Ed. Engl.*, **33**, 1044 (1994).
5) D. R. Kearns, *J. Am. Chem. Soc.*, **91**, 6554 (1969).
6) F. McCapra, *J. Chem. Soc., Chem. Commun.*, **1968**, 155.
7) J. Boche and O. Runquist, *J. Org. Chem.*, **33**, 4285 (1968).
8) a) H. E. O'Neal and W. H. Richardson, *J. Am. Chem. Soc.*, **92**, 6553 (1970); b) H. E. O'Neal and W. H. Richardson, *J. Am. Chem. Soc.*, **93**, 1828 (1971).
9) a) K. Yamaguchi, T. Fueno, and H. Fukutome, *Chem. Phys. Lett.*, **22**, 461 (1973); b) K. Yamaguchi, *Jpn. Chem. Rev.*, **1**, 292 (1973).
10) K. Yamaguchi, *Chem. Phys. Lett.*, **33**, 320 (1975).
11) R. Hilal, *Int. J. Quantum Chem.*, **19**, 805, 821, 833 (1981).
12) L. B. Harding and W. A. Goddard, III, *J. Am. Chem. Soc.*, **99**, 4520 (1977).
13) M. Reguero, F. Bernardi, A. Bottoni, M. Olivucci, and M. A. Robb, *J. Am. Chem. Soc.*, **113**, 1566 (1991).
14) a) J. Y. Koo and G. B. Schuster, *J. Am. Chem. Soc.*, **99**, 5403 (1977); b) K. A. Horn, J. Y. Koo, S. P. Schmidt, and G. B. Schuster, *Mol. Photochem.*, **9**, 1 (1978); c) J. Y. Koo, S. P. Schmidt, and G. B. Schuster, *Proc. Natl. Acad. Sci. U.S.A.*, **75**, 30 (1978); d) G. B. Schuster, B. Dixon, J. Y. Koo, S. P. Schmidt, and J. P. Smith, *Photochem. Photobiol.*, **30**, 17 (1979); e) G. B. Schuster, *Acc. Chem. Res.*, **12**, 366 (1979).
15) a) E. Rapaport, M. W. Cass, and E. H. White, *J. Am. Chem. Soc.*, **94**, 3153, 3160 (1972); b) E. H. White, C. J. Watkins, and E. J. Breaux, *Angew. Chem., Int. Ed. Engl.*, **13**, 229 (1974).
16) a) K. S. V. Santhanam and A. J. Bird, *J. Am. Chem. Soc.*, **87**, 139 (1965); b) N. E. Tokel-Takvoryan, R. E. Hemingway, and A. J. Bird, *J. Am. Chem. Soc.*, **95**, 6582 (1973).
17) a) S. P. Schmidt, M. A. Vincent, C. E. Dykstra, and G. B. Schuster, *J. Am. Chem. Soc.*, **103**, 1292 (1981).
18) a) F. McCapra, *J. Chem. Soc., Chem. Commun.*, **1977**, 946; b) F. McCapra and P. D. Leeson, *J. Chem. Soc., Chem. Commun.*, **1979**, 114.
19) a) K. A. Zaklika, A. L. Thayer, and A. P. Schaap, *J. Am. Chem. Soc.*, **100**, 4916 (1978); b) K. A. Zaklika, T. Kissel, A. L. Thayer, P. A. Burns, and A. P. Schaap, *Photochem. Photobiol.*, **30**, 35 (1979); c) A. P. Schaap and S. D. Gagnon, *J. Am. Chem. Soc.*, **104**, 3504 (1982); d) A. P. Schaap, S. D. Gagnon, and K. A. Zaklika, *Tetrahedron Lett.*, **23**, 2943 (1982).
20) W. Adam, O. Cueto, and F. Yany, *J. Am. Chem. Soc.*, **100**, 2587 (1978).
21) H. Nakamura and T. Goto, *Photochem. Photobiol.*, **30**, 27 (1979).
22) C. Lee and L. A. Singer, *J. Am. Chem. Soc.*, **102**, 3823 (1980).
23) K. Yamaguchi, in "Singlet Oxygen Vol. III, Reaction Models and Products," Part 2, ed by A. A. Frimer, CRC Press, Boca Raton, Florida (1985), p. 119.
24) L. H. Catalani and T. Wilson, *J. Am. Chem. Soc.*, **111**, 2633 (1989).
25) a) A. P. Schaap, T. -S. Chen, R. S. Handley, R. DeSilva, and B. P. Giri, *Tetrahedron Lett.*, **28**, 1155 (1987); b) A. P. Schaap, M. D. Sandison, and R. S. Handley, *Tetrahedron Lett.*, **28**, 1159 (1987).
26) a) I. Bronstein, B. Edwards, and J. Voyta, *J. Biolumin. Chemilumin.*, **2**, 186 (1988); b) I. Bronstein, J. Voyta, G. Thorpe, and L. Kricka, *Clin. Chem.*, **35**, 1441 (1989); c) B. Edwards, A. Sparks, J. C. Voyta, R. Strong, O. Murphy, and I. Bronstein, *J. Org. Chem.*, **55**, 6225 (1990).
27) a) M. Matsumoto, H. Suganuma, Y. Katao, and H. Mutoh, *J. Chem. Soc., Chem. Commun.*, **1995**, 431; b) M. Matsumoto, N. Watanabe, H. Kobayashi, M. Azami, and H. Ikawa, *Tetrahedron Lett.*, **38**, 411 (1997); c) M. Masakatsu, N. Watanabe, N. C. Kasuga,

F. Hamada, and K. Tadokoro, *Tetrahedron Lett.*, **38**, 2863 (1997); d) M. Matsumoto, N. Arai, and N. Watanabe, *Tetrahedron Lett.*, **37**, 8535 (1996); e) M. Matsumoto, N. Watanabe, T. Shino, H. Suganuma, and J. Matsubara, *Tetrahedron Lett.*, **38**, 5825 (1997); f) M. Matsumoto, N. Watanabe, H. Kobayashi, H. Suganuma, J. Matsubara, Y. Kitano, and H. Ikawa, *Tetrahedron Lett.*, **37**, 5939 (1996).

28) M. Kimura, H. Nishikawa, H. Kura, H. Lim, and E. H. White, *Chem. Lett.*, **1993**, 505.

29) Y. Yoshioka, S. Yamanaka, S. Yamada, T. Kawakami, M. Nishino, K. Yamaguchi, and A. Nishinaga, *Bull. Chem. Soc. Jpn.*, **69**, 2701 (1996).

30) W. Hiller, A. Nishinaga, and A. Rieker, *Z. Naturforsch., B*, **47b**, 1185 (1992).

31) F. McCapra, I. Beheshti, A. Bunford, R. A. Hann, and K. A. Zaklika, *J. Chem. Soc., Chem. Commun.*, **1977**, 944.

32) S. W. Benson and P. S. Nangia, *J. Am. Chem. Soc.*, **102**, 2844 (1980).

33) K. Yamaguchi, K. Takada, Y. Otsuji, and K. Mizuno, in "Organic Peroxides," ed by W. Ando, John Wiely, New York (1992), p. 2.

34) N. J. Turro and A. Devaquet, *J. Am. Chem. Soc.*, **97**, 3859 (1975).

35) a) Y. Yoshioka, T. Tsunesada, K. Yamaguchi, and I. Saito, *Int. J. Quantum Chem.*, **65**, 787 (1997); b) Both MP4 and CCSD-(T)//MP2 6-31G* calculations were performed for the locations of transition structures and intermediates in the decomposition process of dioxetane. Detailed state correlation diagrams will be published sooner.

36) W. Adam, A. Beinhauer, and H. Hauer, in "CRC Handbook of Photochemistry," ed by J. C. Scaiano, CRC Press, Boca Raton, FL (1989), Vol. II, p. 271.

37) L. N. Domelsmith, L. L. Munchausen, and K. N. Houk, *J. Am. Chem.Soc.*, **99**, 4311 (1977).

38) A. A. Gorman, G. Lovering, and M. A. J. Rogers, *J. Am. Chem. Soc.*, **101**, 3050 (1979).

39) M. J. Thomas and C. S. Foote, *Photochem. Photobiol.*, **27**, 683 (1978).

40) a) D. Rehm and A. Weller, *Ber. Bunsenges. Physik. Chem.*, **73**, 834 (1969); b) D. Rehm and A. Weller, *Isr. J. Chem.*, **8**, 259 (1970).

41) R. A. Marcus, *J. Chem. Phys.*, **24**, 3047 (1956).

42) C. Kemal and T. C. Bruice, *J. Am. Chem. Soc.*, **99**, 7064 (1977).